JACS
JOURNAL OF THE AMERICAN CHEMICAL SOCIETY

Article

pubs.acs.org/JACS

Substrate-Assisted and Nucleophilically Assisted Catalysis in Bovine α1,3-Galactosyltransferase. Mechanistic Implications for Retaining Glycosyltransferases

Hansel Gómez,[‡,†] José M. Lluch,[‡,†] and Laura Masgrau*[,‡]

[‡]Institut de Biotecnologia i de Biomedicina and [†]Department of Chemistry, Universitat Autònoma de Barcelona, 08193 Bellaterra (Cerdanyola del Vallès), Barcelona, Spain

Supporting Information

ABSTRACT: Glycosyltransferases (GTs) are responsible for the biosynthesis of glycans, the most abundant organic molecules in nature. Their biological relevance makes necessary the knowledge of their catalytic mechanism, which in the case of retaining GTs is still a matter of debate. After the initial proposal of a double-displacement mechanism with formation of a covalent glycosyl−enzyme intermediate (CGE), new experimental and computational data are pointing out to a front-side attack as a plausible alternative. The question is then why family GT6 members, like bovine α1,3-galactosyltransferase (α1,3-GalT), have a nucleophilic residue (Glu317) situated close to the anomeric carbon. To answer this and other questions, QM(DFT)/MM calculations on the entire α1,3-GalT:substrates system (and for the E317A/E317Q mutants) have been carried out. We describe a substrate-assisted mechanism for retaining GTs consisting of the stabilization of the developing negative charge on the β-phosphate by the hydrogen of the attacking hydroxyl group of the acceptor molecule. This interaction is impaired in the α1,3-GalT reactants, which explains why Glu317 is required to nucleophilically assist initial catalysis by "pushing" leaving-group departure. The presence of Glu317 opens the door to the possibility of a double-displacement mechanism in GT6 family. Our results suggest that in α1,3-GalT the substrate-assisted catalysis would be necessary in both mechanisms (for which we predict similar reaction rates), because the nucleophilic strength of Glu317 is reduced by the interactions it makes to ensure proper acceptor binding. Interestingly, the same effect would be found in the absence of the acceptor when Glu317 interacts with water molecules, which could explain the difficulties for isolating the CGE experimentally, and could be a strategy to avoid undesired hydrolysis of the donor substrate.

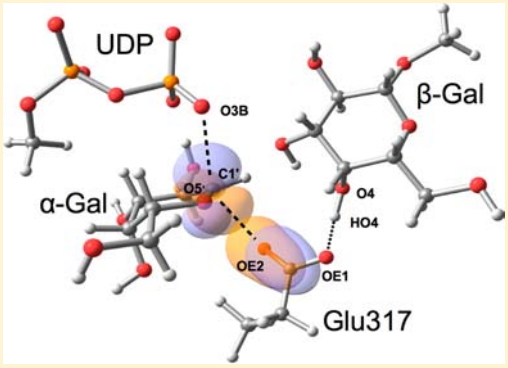

INTRODUCTION

Glycans (mono-, oligo-, and polysaccharides and their conjugates) are ubiquitous in all organisms and the most abundant organic molecules on Earth. They participate in a variety of biological functions including cellular and molecular recognition, energy storage, and structural stability. Moreover, they exhibit properties that are known to be useful in a large array of applications (e.g., biofuel, biomaterials, disease markers, or tissue engineering). In nature, glycan synthesis is performed by glycosyltransferases (GTs), a highly stereo- and regiospecific class of enzymes for which the reaction mechanism is still not well understood and neither are the factors assisting catalysis. A detailed understanding of their mechanism would benefit both the rational design of specific inhibitors for those GTs that are therapeutic targets and the use of GTs in biotechnology (e.g., for the synthesis of a wide range of glycosylated molecules).

In the present work we focus on the study of retaining GTs, that is, GTs that catalyze the transfer of a monosaccharide from an activated donor to an acceptor molecule with net retention of the configuration at the anomeric carbon.

Today there is a wide-open debate around the mechanistic details of this type of enzymes.[1−10] By analogy with retaining glycosidases (GHs), and despite an evident lack of evolutionary relatedness,[11] catalysis by retaining GTs was initially proposed to proceed via a double-displacement mechanism with the formation and subsequent cleavage of a covalent glycosyl−enzyme intermediate (CGE) (Scheme 1A). Clearly, this mechanism requires the presence of an appropriately positioned nucleophile within the active site. Several experiments are in agreement with such a mechanism, although conclusive evidence for the formation of a CGE in the wild-type enzymes has been elusive for many years, even in those GTs for which a possible nucleophile has been identified. In particular, a CGE was detected for the Q189E:UDP-2′FGal complex of lipopolysaccharyl-α1,4-galactosyltransferase C (LgtC, family GT8),[12] but Asp190 was involved instead of the putative nucleophile at position 189. For the human ABO(H) blood group glycosyltransferases (family GT6), a CGE has recently

Received: March 8, 2013
Published: April 11, 2013

   dx.doi.org/10.1021/ja4024447 | J. Am. Chem. Soc. 2013, 135, 7053−7063

Scheme 1. Proposed Mechanisms for the Retaining GTs with a Putative Nucleophile in the Active Site[a]

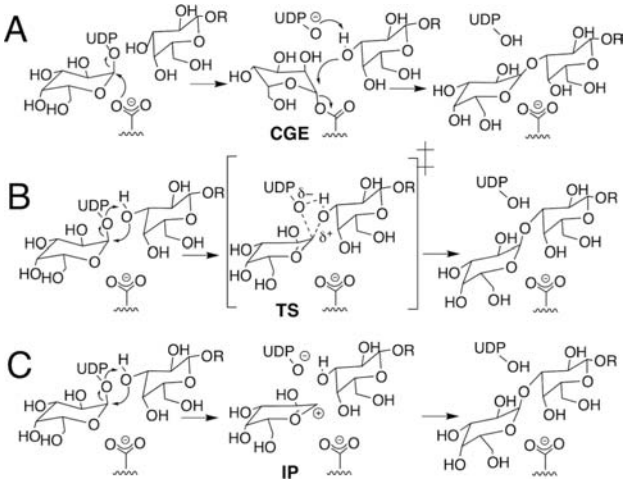

[a](A) Double-displacement mechanism with formation of a covalently bound glycosyl−enzyme intermediate (CGE). (B) Front-side single-displacement mechanism (S_Ni) with formation of an oxocarbenium ion-like transition state (TS). (C) Front-side attack mechanism (S_Ni-like) with formation of a short-lived oxocarbenium−phosphate ion pair intermediate (IP).

been characterized for the E303C mutant in the absence of the acceptor substrate.[3] In contrast, for bovine α1,3-galactosyltransferase (α1,3-GalT), another GT6 family member with a suitable positioned glutamate in the active site, E317C mutation did not lead to the identification of a CGE;[13] E317D, E317C, E317A,[13] and E317Q[14] mutants showed residual activities of 0.04−0.8%, and, for the E317A mutant, partial recovery of activity was achieved by chemical rescue with azides.[1] These data were interpreted as consistent with the double-displacement mechanism.

The availability of an increasing number of crystal structures has shown that in most retaining GTs there is not a well-positioned residue in the active site to act as the nucleophile.[2] In fact, only for family GT6 has a suitable nucleophile been described. Moreover, given the structural conservation of the different binary complexes solved (either with the donor or with the acceptor substrate), it seems improbable that they do not correspond to the catalytically competent enzyme's overall conformation. Therefore, an alternative mechanism involving retention of the configuration is being put forth, that is, a front-side attack of the acceptor nucleophile on the same side as the leaving group with formation of an oxocarbenium ion-like transition state (S_Ni, or A_ND_N according to the IUPAC nomenclature, Scheme 1B), or even an oxocarbenium−phosphate short-lived ion pair (IP) intermediate (S_Ni-like, or $D_N{*}A_N$, Scheme 1C). The latest theoretical and experimental works on retaining GTs[4−6,8,9,15] are giving support to this front-side attack mechanism, either S_Ni or S_Ni-like, at least for those retaining GTs where no good nucleophile is suitably positioned to form the CGE. In this mechanism, the presence of a nucleophile on the β-face of the sugar ring could facilitate catalysis by "pushing" the leaving group.[2,9] A third type of mechanism involving elimination/addition steps through a non-covalently bound intermediate bearing a C1′−C2′ double bond has very recently been proposed as a possible alternative from the study of *Pyrococcus abissi* glycogen synthase.[10]

At the present stage of investigation there are several pending questions to be clarified, especially for those enzymes where a well-positioned nucleophile has been identified. First, it is necessary to know whether GT6 family members follow a double-displacement mechanism or not. Second, the exact role of this glutamate/aspartate residue in the vicinity of the anomeric center needs to be identified. Third, it is important to understand why assistance by the nucleophile would be required for these enzymes but not for others. Finally, a deeper theoretical study of the CGE formation is desirable in an attempt to rationalize the difficulties found to isolate it (if formed) experimentally.

In this paper, we present a detailed full-enzyme hybrid quantum mechanics/molecular mechanics (QM/MM) study of the GT6 member α1,3-GalT and try to give answer to the above questions. In a preliminary study we proposed that Glu317 would have an essential role even in the case of a front-side attack mechanism, but the level of theory used did not permit a more quantitative analysis. Here the methodology is improved by using higher levels of theory to explore the potential energy surface of the system and more protein conformations. Moreover, mutant enzymes are also studied, a detailed comparison with LgtC (which catalyzes reaction between the two same substrates) is done, and Natural Bond Population analysis is carried out to examine the relevance of substrate-assisted catalysis in these systems and the nucleophilic strength of Glu317 in α1,3-GalT. At the end, the mechanistic implications for retaining GTs are discussed.

MODELS AND METHODS

Coordinates from the X-ray structure (PDB code 1O7O,[14] resolution 1.97 Å) were considered as starting point to model the Michaelis complex of the enzyme with its ligands (α1,3-GalT + M^{2+} + UDP−Gal + LAT). (See Supporting Information (SI), section 1, for further details on the modeling procedure.) As explained in the SI, Mg^{2+} was used instead of Mn^{2+}. All the crystallographic water molecules present in the 1O7O structure, excluding those overlapping (within 4 Å) with the modeled UDP−Gal, were considered in the setup of the initial complex. The system was fully solvated with a cubic box of TIP3P water molecules (83 × 77 × 73 $Å^3$), and one Cl^- ion was added to neutralize the system using VMD version 1.8.9.12.[16] The same program was used to generate the mutants of the enzyme as well as the figures showing molecular structures.

Starting from this model of the ternary complex, we performed 5 ns of classical molecular dynamics (MD) simulation at 300 K using the CHARMM22 force field[17−19] and periodic boundary conditions, as implemented in the NAMD software.[20] Specific topology and parameters from the CHARMM force field for carbohydrates were considered.[21] Afterward, a 80 ps QM(SCC-DFTB[22,23])/CHARMM22 MD was performed, and four snapshots were randomly selected as starting points for subsequent QM(DFT)/MM calculations. All residues and water molecules within 15 Å of the anomeric center (2089 atoms) were included in the active region (see Figure 1 and SI for more details). The charge of the QM region was −3 and included 84 atoms: those from the α- and β-galactose rings from UDP−Gal and LAT, respectively, Mg^{2+} and its first coordination sphere (phosphate groups from UDP and the side chains of residues Asp225, Asp227 and a crystallographic water), as well as the side chain of Glu317 (see Scheme 2).

Reaction paths were scanned by performing constrained QM-(BP86[24−27]/SVP[28])/CHARMM optimizations along suitably defined reaction coordinates in steps of 0.2 Å that provided us the starting structures for subsequent full optimization of all the relevant stationary points (i.e., reactants, transition states, covalent intermediates, and products). We have used this level of calculation before for geometry optimizations in a previous work on LgtC[8] and showed that it

dx.doi.org/10.1021/ja4024447 | J. Am. Chem. Soc. 2013, 135, 7053−7063

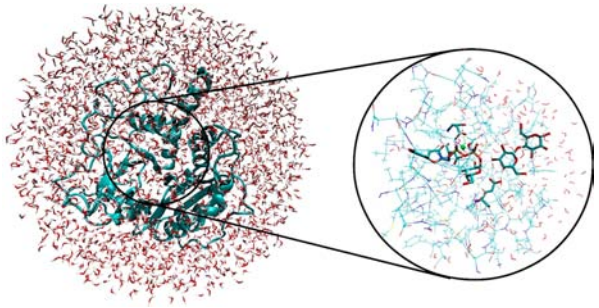

Figure 1. Model system used in the QM/MM calculations. The active region is enlarged and the QM atoms represented in licorice.

Scheme 2. QM/MM Partition Used in the Present Study[a]

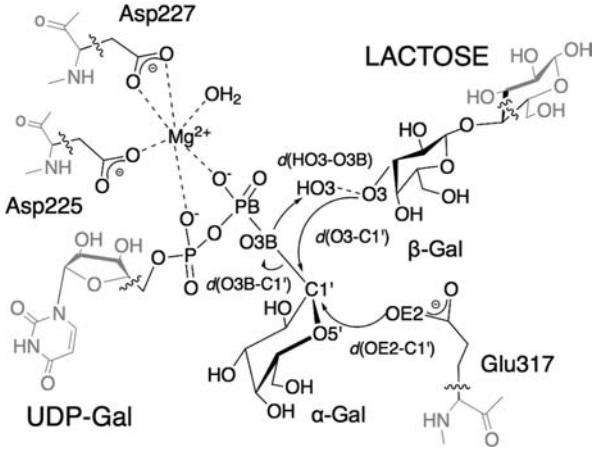

[a]QM and MM atoms are depicted in black and gray, respectively. Wavy lines indicate the boundary between the QM and MM regions. The arrows indicate the distances considered in the reaction coordinates, and the atoms involved are labeled.

provided with fairly good geometries while saving computational time, thanks to the use of the resolution-of-the-identity (RI) approximation.[29,30] Frequency calculations were performed for the QM region to confirm that the optimized TS structures are indeed characterized by one imaginary frequency and a suitable transition vector. Additional single-point energy calculations were carried out at the M05-2X[31]/TZVP[32] level which has proven to properly describe retaining GT systems.[8,33,34] For the purpose of comparison, additional single-point energies were calculated at the BP86/TZVP, B3LYP/SVP, and B3LYP/TZVP levels of theory (see SI, section 2.1).

The electrostatic stabilization provided by different residues to the QM(M05-2X/TZVP)/CHARMM energy was examined by setting their point charges to zero in additional single-point energy calculations. A Natural Bond Orbital (NBO) analysis[35−38] was also performed for some of the stationary points using the NBO program v3.1[39] included in Gaussian09.[40]

All QM/MM calculations were performed with the modular program package ChemShell,[41] using TURBOMOLE[42] or Gaussian09 at the DFT level (BP86, B3LYP[24,26,43−45] and M05-2X functionals) or MNDO[46] at the SCC-DFTB level. MM energies and gradients were retrieved from DL_POLY,[46] using the CHARMM force field. An electronic embedding scheme[47] was adopted in the QM/MM calculations, and no cutoffs were introduced for the nonbonding MM and QM/MM interactions. Six hydrogen link atoms were employed to treat the QM/MM boundary with the charge shift model.[48,49] Energy minimizations were done with the low-memory Broyden−Fletcher−Goldfarb−Shanno (L-BFGS) algorithm,[50,51] and the TS searches were performed with the microiterative TS optimizer that combines L-BFGS and the partitioned rational function optimizer (P-RFO).[52,53] Both L-BFGS and P-RFO algorithms are implemented in the HDLCopt[54] module of ChemShell.

RESULTS AND DISCUSSION

Catalytic Mechanism of α1,3-GalT: Double Displacement vs Front-Side Attack. We have tested several reaction coordinates (RCs) to model the different mechanistic alternatives for the transfer of α-Gal from UDP−Gal to LAT by α1,3-GalT (Scheme 1). A double-displacement mechanism was first considered. The RC = $[d(\mathrm{O3B_{UDP}}-\mathrm{C1'_{\alpha\text{-}Gal}}) - d(\mathrm{OE2_{E317}}-\mathrm{C1'_{\alpha\text{-}Gal}}) - d(\mathrm{HO3_{\beta\text{-}Gal}}-\mathrm{O3B_{UDP}})]$ was needed for the first step of the reaction in order to properly model the CGE formation; the RC = $[d(\mathrm{OE2_{E317}}-\mathrm{C1'_{\alpha\text{-}Gal}}) - d(\mathrm{O3_{\beta\text{-}Gal}}-\mathrm{C1'_{\alpha\text{-}Gal}}) - d(\mathrm{HO3_{\beta\text{-}Gal}}-\mathrm{O3B_{UDP}})]$ was used for the following attack of LAT on the anomeric center (Schemes 1A and 2). All the stationary points (reactants, transition states, intermediates and products) were then characterized. The QM/MM potential energy barriers and reaction energies calculated at the QM=(M05-2X/TZVP//BP86/SVP) level for the four frames considered are summarized in Figure 2A. Notice that, unless

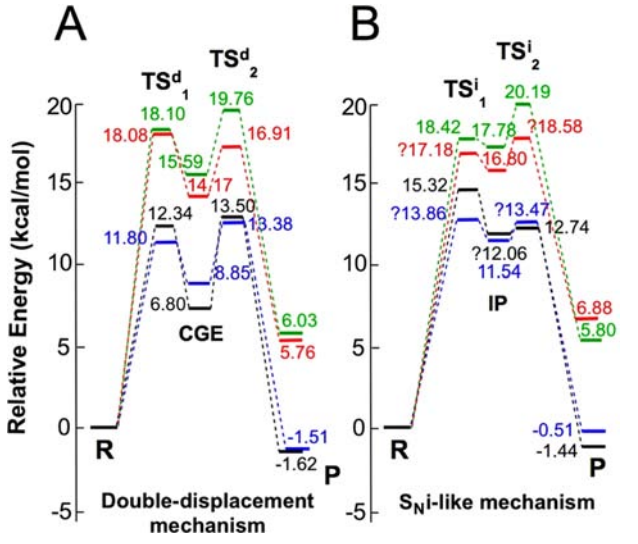

Figure 2. QM/CHARMM potential energy barriers and reaction energies for α1,3-GalT. QM=M05-2X/TZVP//BP86/SVP. (A) Double-displacement mechanism. (B) *Nucleophilically assisted* S_Ni-like mechanism. The ? indicate that the TS or IP nature of this stationary point could not be confirmed by the frequency calculation. Blue, black, red, and green lines correspond to the frames considered in the present study as starting points for the QM/MM calculations (frames 1−4, respectively).

otherwise indicated, we will be considering the QM=(M05-2X/TZVP//BP86/SVP) level of theory, which is expected to provide the most reliable energy data (see Models and Methods section). A more detailed comparison of the energies calculated at different levels is available in the SI (see section 2.1 and Tables S1−S4). Also, notice that two groups of potential energy barriers can be distinguished in Figure 2: those from frames 1-2 and 3-4, respectively. They correspond to two subsets of structures differing in the initial orientation of a water molecule interacting with UDP (see SI section 2.2 for more details).

The average potential energy barriers for formation and subsequent cleavage to products of the CGE are quite similar (15.1 ± 3.5 and 15.9 ± 3.1 kcal/mol, respectively, both measured with respect to the reactants), and are also quite

dx.doi.org/10.1021/ja4024447 | J. Am. Chem. Soc. 2013, 135, 7053−7063

Table 1. Selected QM/MM Bond Distances d (Å) and Atomic Charges q (au) in the Optimized Reactants (R), Transition States (TS), Ion Pair Intermediate (IP), and Products (P) for the Double-Displacement and S_Ni-like Mechanisms for Frame 2[a]

		double-displacement mechanism				nucleophilically assisted S_Ni-like mechanism			
	R	TS^d_1	CGE	TS^d_2	P	TS^i_1	?IP[b]	TS^i_2	P
$d(O3B_{UDP}-C1'_{\alpha\text{-Gal}})$	1.51	3.18	3.95	3.45	3.45	2.48	3.40	3.59	3.40
$d(O3_{\beta\text{-Gal}}-C1'_{\alpha\text{-Gal}})$	3.04	2.85	3.09	2.49	1.48	2.87	2.79	2.63	1.48
$d(HO3_{\beta\text{-Gal}}-O3_{\beta\text{-Gal}})$	1.00	1.02	1.02	1.03	1.51	1.01	1.02	1.03	1.51
$d(HO3_{\beta\text{-Gal}}-O3B_{UDP})$	4.06	1.58	1.59	1.51	1.04	1.63	1.57	1.52	1.04
$d(OE2_{E317}-C1'_{\alpha\text{-Gal}})$	4.25	2.60	1.56	2.77	3.18	3.16	2.51	2.61	3.19
$d(C1'_{\alpha\text{-Gal}}-O5'_{\alpha\text{-Gal}})$	1.38	1.28	1.37	1.28	1.40	1.28	1.28	1.28	1.40
$q(C1'_{\alpha\text{-Gal}})$	0.36	0.58	0.35	0.58	0.32	0.57	0.58	0.58	0.32
$q(O5'_{\alpha\text{-Gal}})$	−0.51	−0.40	−0.52	−0.41	−0.53	−0.41	−0.41	−0.41	−0.54

[a]QM = BP86/SVP and M05-2X/TZVP//BP86/SVP for the distances and charges, respectively. [b]The ? indicates that the IP intermediate was not supported by the frequency calculation.

similar within a given frame. These results are in qualitative agreement with the corresponding experimentally derived phenomenological free energy barrier of ∼17 kcal/mol (k_{cat} = 6.4 s^{-1} at 310 K),[55] and would give theoretical support to the double-displacement mechanism hypothesis for this enzyme−substrate system. As can be seen in Figure 2A, CGE formation is quite endoergic (the CGE lays 11.4 ± 4.2 kcal/mol over the reactants), and the barrier for going back to the reactants is relatively small (3.7 ± 1.3 kcal/mol).

The evolution of some key distances along this reaction path is similar for the four frames considered. The values corresponding to the selected frame are listed in Table 1. (From now on, given the similar results obtained for the four frames and in order to facilitate the discussion, only the results of frame 2 will be reported and discussed in the main text. See SI Tables S5−S7 for the other frames.) Essentially, in the transition state of the first step (TS^d_1) the bond between the UDP leaving group and the α-Gal is already broken ($d(O3B_{UDP}-C1'_{\alpha\text{-Gal}})$ > 2.5 Å) while the Glu317 OE2 atom is still at 2.6 Å from the anomeric center. These distances are 3.95 Å and 1.56 Å at the CGE, respectively. In the transition state of the second step (TS^d_2), $d(OE2_{E317}-C1'_{\alpha\text{-Gal}})$ = 2.77 Å and $d(O3_{\beta\text{-Gal}}-C1'_{\alpha\text{-Gal}})$ = 2.49 Å, which indicates that the CGE has already dissociated while the incoming hydroxyl group from LAT is still approaching the anomeric center. Thus, both TSs present a highly dissociative character. The TSs and CGE structures are shown in the SI (Figure S1).

The front-side attack mechanism was considered next. For that, the RC = $[d(O3B_{UDP}-C1'_{\alpha\text{-Gal}}) - d(O3_{\beta\text{-Gal}}-C1'_{\alpha\text{-Gal}}) - d(HO3_{\beta\text{-Gal}}-O3B_{UDP})]$ was used to obtain the starting points for TSs and intermediate search and characterization. The energy barriers and reaction energies calculated for α1,3-GalT appear summarized in Figure 2B. For this mechanism, corresponding to the S_Ni-like depicted in Scheme 1C, we were able to find a (short-lived) IP intermediate. The TSs and IP structures are shown in the SI (Figure S2).

Again, the transition states for the first and second steps (TS^i_1 and TS^i_2, respectively) are very similar in average energy (16.2 ± 2.0 and 16.3 ± 3.7 kcal/mol, respectively) and are in the range of the experimentally derived ones. The IP lays 14.6 ± 3.2 kcal/mol over the reactants and between 0.6 and 3.2 kcal/mol below the two TSs (depending on the frame), indicating its short-lived nature. Inspection of Table 1 reveals that, again, the two TSs are very dissociative and that TS^i_1, IP and TS^i_2 exhibit very similar bond distances. In particular, changes >0.1 Å are only seen for $d(O3_{\beta\text{-Gal}}-C1'_{\alpha\text{-Gal}})$ (change of 0.24 Å), $d(OE2_{E317}-C1'_{\alpha\text{-Gal}})$ (0.65 Å), and $d(O3B_{UDP}-C1'_{\alpha\text{-Gal}})$ (1.1 Å), which is the leaving group−sugar bond. This flat character of the potential energy surface zone describing all these oxocarbenium-like species can be clearly seen in the two-dimensional QM(BP86/SVP)/CHARMM potential energy surface depicted in Figure 3. To build this PES, from every

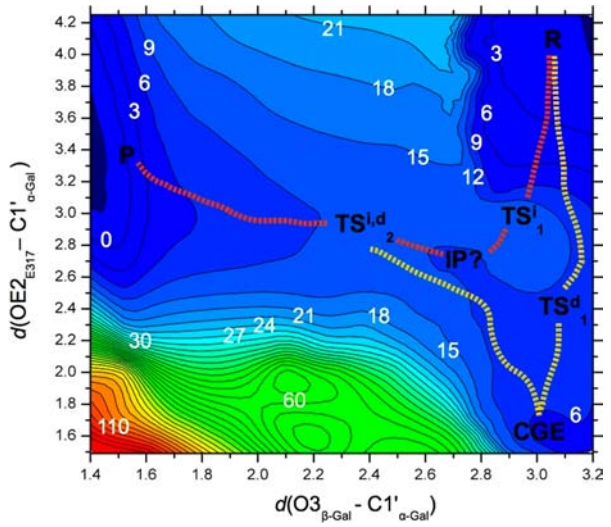

Figure 3. Two-dimensional QM(BP86/SVP)/CHARMM potential energy surface for frame 2. Energies are given in kcal/mol and distances in Å. Contour lines are drawn at intervals of 3 kcal/mol.

structure coming from the reaction path used to model the CGE formation (RC = $[d(O3B_{UDP}-C1'_{\alpha\text{-Gal}}) - d(OE2_{E317}-C1'_{\alpha\text{-Gal}}) - d(HO3_{\beta\text{-Gal}}-O3B_{UDP})]$) we fixed $d(OE2_{E317}-C1'_{\alpha\text{-Gal}})$ and simulated a front-side attack mechanism (RC = $[d(O3B_{UDP}-C1'_{\alpha\text{-Gal}}) - d(O3_{\beta\text{-Gal}}-C1'_{\alpha\text{-Gal}}) - d(HO3_{\beta\text{-Gal}}-O3B_{UDP})]$). For clarity, only $d(OE2_{E317}-C1'_{\alpha\text{-Gal}})$ and $d(O3_{\beta\text{-Gal}}-C1'_{\alpha\text{-Gal}})$ are represented in the y- and x-axis, respectively. The reactants and products minima are located at the top-right corner and the middle-left border, respectively. Two possible pathways connect them: one going through the CGE, and the other one corresponding to the S_Ni-like mechanism. Notice the well-defined flat zone (within a range of 2−3 kcal/mol) surrounding the IP, which evidences the idea that the different oxocarbenium-like species have very similar potential energies. In addition, notice that TS^i_2 and TS^d_2 are geometrically very similar. This flatness of the PES is probably the reason why a systematic validation of all the IP and TSs by frequency calculations has not always been possible.

dx.doi.org/10.1021/ja4024447 | J. Am. Chem. Soc. 2013, 135, 7053−7063

In our preliminary work on the α1,3-GalT mechanism,[9] a single TS corresponding to the S_Ni mechanism (Scheme 1B) was characterized and no IP could be found; these differences with the present work are probably because at that time the initial exploration of the PES was carried out at the SCC-SFTB/CHARMM level of calculation. In principle, we are more confident with the present results as we have applied a higher level of theory and we have sampled over different enzyme−substrates configurations. Still, even more definitive conclusions could be drawn if the 2D free energy surface was available.[56,57] Nevertheless, in systems presenting an energy topology with these characteristics the difference between a S_Ni and a S_Ni-like mechanism may be quite subtle and, thus, it is difficult to assess both from theoretical and experimental methods. Fortunately, the energetic and structural similarities between the oxocarbenium species found for this system suggests that such strict differentiation between these two mechanisms may actually be irrelevant from a more general and practical point of view.

On the other hand, the comparison between the double-displacement and front-side attack mechanisms is of much more interest. Averaging over the different frames the highest energy barrier calculated in each case, we obtain barrier heights of 16.2 ± 3.2 and 16.9 ± 2.9 kcal/mol for the double displacement and the front-side attack, respectively. Both values are very similar and in agreement with the experimentally derived phenomenological free energy of activation (∼17 kcal/mol). In conclusion, our new results suggest that for α1,3-GalT both mechanisms could be acting at the same time in a competitive or complementary manner.

A detailed analysis of the factors modulating catalysis is presented in the next subsections.

Nucleophilically Assisted Catalysis in α1,3-GalT. As mentioned in the Introduction, experimental mutations of the active site nucleophile, Glu317, pointed to a double-displacement mechanism for α1,3-GalT, although they could not completely rule out other possibilities. Moreover, Glu317 has also been described to participate in acceptor binding.[14] It is obvious that Glu317 mutation would disrupt the reaction in the case of a double displacement.

Remarkably, looking at the changes in $d(OE2_{E317}-C1'_{\alpha\text{-Gal}})$ for the front-side attack (Table 1 and Figure 3) it becomes apparent that in this mechanism Glu317 is also participating in catalysis ($d(OE2_{E317}-C1'_{\alpha\text{-Gal}})$ = 4.25, 3.16, 2.51, and 2.61 Å in R, TS^i_1, IP, and TS^i_2, respectively). This trend was already observed in our previous work,[9] where we proposed that for α1,3-GalT Glu317 would also be crucial in a front-side attack mechanism.

To shed more light on the role of Glu317, we decided to perform a more quantitative analysis here by modeling the front-side attack mechanism for the *in silico* E317A and E317Q mutants. As shown in Figure 4, much sharper energy profiles are obtained for the mutants when compared to the WT enzyme, and only one maximum is identified (S_Ni mechanism, Scheme 1B). The energy barriers corresponding to the TSs are 30.9 and 26.0 kcal/mol for the E317A and E317Q mutants, respectively. This destabilization of the TSs relative to the reactants correlates with a worst stabilization of the positive charge on the α-Gal ring, which makes UDP departure less favorable. Therefore, it is confirmed that even in the case of a front-side attack mechanism the role of Glu317 is very noticeable, which could also explain the mutagenesis experimental results. As anticipated by Lairson et al.,[2] a

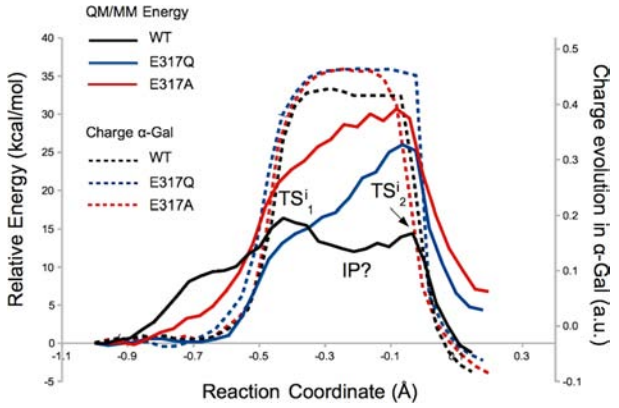

Figure 4. QM(M05-2X/TZVP//BP86/SVP)/CHARMM energy profiles along the $d(O3B_{UDP}-C1'_{\alpha\text{-Gal}}) - d(O3_{\beta\text{-Gal}}-C1'_{\alpha\text{-Gal}}) - d(HO3_{\beta\text{-Gal}}-O3B_{UDP})$ reaction coordinate for the wild-type enzyme and the E317A and E317Q mutants. The charge evolution at the α-Gal ring along the reaction is depicted as dashed lines.

nucleophile in the back side could "push" the UDP leaving group to form an IP intermediate. In that sense, our current and previous findings suggest that some retaining GTs may actually require a strong nucleophile on the β-face of the donor sugar substrate, without necessarily involving the formation of a CGE, but in a *nucleophilically assisted* front-side attack mechanism. Again, such mechanism will only be possible for those retaining GTs presenting a well positioned nucleophile in the active site. In these cases, and as showed by the present study, it is likely that both mechanisms are not exclusive but complementary.

UDP−Gal Bond Cleavage. Comparison between α1,3-GalT and LgtC. Why would some retaining GTs require a nucleophile in the β-face of the donor sugar substrate to facilitate the leaving-group (UDP) departure? In other words, is UDP−sugar bond cleavage more difficult in some retaining GTs than in others? Notice that in all the proposed mechanisms the beginning of the reaction is dominated by UDP−Gal bond cleavage. Thus, to get some answers to these questions we have compared the leaving-group departure process in the ternary complex for two retaining GTs: α1,3-GalT and LgtC. LgtC catalyzes the reaction between the same substrates (UDP−Gal and LAT) but has a glutamine (Gln189) in the place of Glu317(α1,3-GalT).[8,15,58] Previous theoretical studies of LgtC have concluded that it follows a S_Ni mechanism and have not found any evidence of a double-displacement mechanism.[8,15]

The QM/MM energy profiles for UDP−Gal bond cleavage are depicted in Figure 5A. Surprisingly, and despite the presence of Glu317, bond cleavage following the $d(O3B_{UDP}-C1'_{\alpha\text{-Gal}})$ coordinate is much more difficult in α1,3-GalT than in LgtC. In our previous work on LgtC, only a moderate electrostatic stabilization of the TS by Gln189 was estimated (∼2 kcal/mol).[8] In α1,3-GalT, Glu317 was expected to provide a better stabilization of the positive charge developed in α-Gal, but apparently its contribution is not *enough* to make the bond breakage sufficiently easy. It is important to remind here that, despite this difference in bond cleavage, the two enzymes exhibit similar experimentally and theoretically derived energy barriers (∼17 kcal/mol for α1,3-GalT and ∼16 kcal/mol for LgtC[8]). One of the main goals of the present study is then to clarify this alleged inconsistency that we have found in the bond-breakage readiness when comparing α1,3-GalT and LgtC.

dx.doi.org/10.1021/ja4024447 | J. Am. Chem. Soc. 2013, 135, 7053−7063

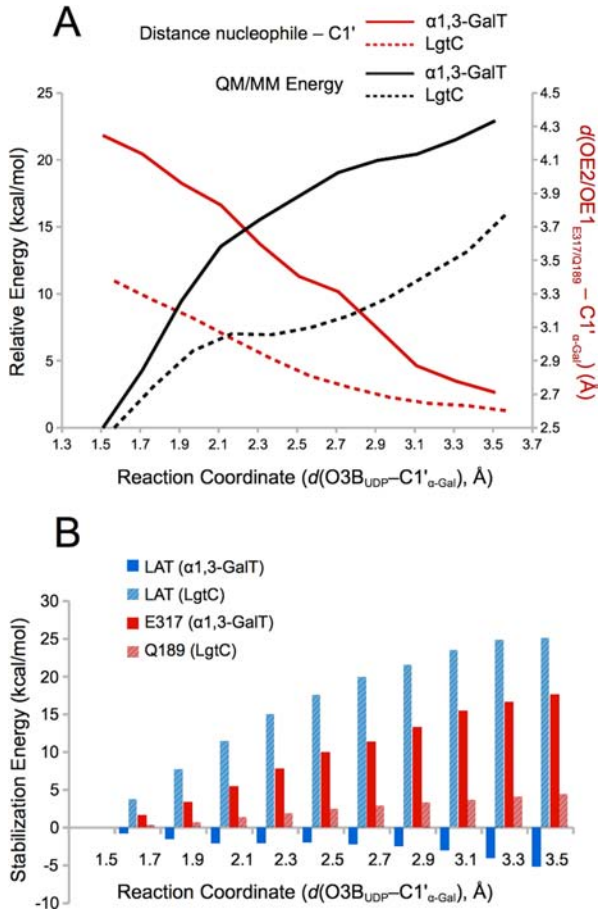

Figure 5. Comparative analysis of the bond-breakage process in α1,3-GalT and LgtC at the QM(M05-2X/TZVP//BP86/SVP) level of calculation. (A) Energy profile for the bond-breakage process and variation of the d(OE2/OE1$_{E317/Q189}$–C1′$_{\alpha\text{-Gal}}$) distance. (B) Electrostatic contribution to the stabilization of the QM region by the acceptor substrate (LAT) and the active-site nucleophile (Glu317 or Gln189 in α1,3-GalT or LgtC, respectively).

We started by analyzing the charge evolution in the donor substrate as the O3B$_{UDP}$–C1′$_{\alpha\text{-Gal}}$ bond is broken (Figure S4). The positive charge development on α-Gal is very similar for both enzymes, whereas α1,3-GalT develops a higher negative charge on UDP (−0.51 vs −0.41 au). The data in Figure 5, thus, indicate that although it has always been suggested that stabilization of the anomeric carbon positive charge is a key factor in glycosyl transfer, stabilization of the charge on the UDP leaving group is also crucial and it seems to be making an important difference between these two enzymes.

Contribution from the Enzyme's Residues. An analysis of the active site residues capable of stabilizing this charge development was performed. We calculated, for all the residues in the active space, their electrostatic contribution to the stabilization of the QM region as the O3B$_{UDP}$–C1′$_{\alpha\text{-Gal}}$ bond is broken. The contribution from the putative nucleophile (Glu317 or Gln189) is shown in Figure 5B. Other residues that contribute significantly are depicted in Figure 6 (see also SI, Table S9). As can be seen, the contribution of Glu317 in α1,3-GalT is much more significant (4 times higher) than that of Gln189 in LgtC. Curiously, we found more stabilizing residues in the active site of α1,3-GalT than in LgtC, most of them localized in the upper face of the UDP–Gal. Thus, according to the different stabilization of the negative charge on

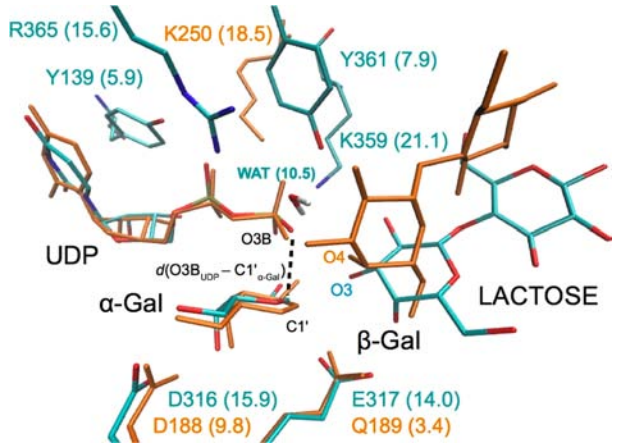

Figure 6. O3B$_{UDP}$–C1′$_{\alpha\text{-Gal}}$ bond-breakage process. Main electrostatic contributions (kcal/mol) of residues in the active site of α1,3-GalT (cyan) and LgtC (orange) to the stabilization of the QM region. The reactants and a structure with d(O3B$_{UDP}$–C1′$_{\alpha\text{-Gal}}$) ≈ 3 Å were considered to compute the energy differences with the reactants.

the UDP provided by the enzyme's residues, bond cleavage in α1,3-GalT would be expected to be easier than in LgtC.

Inter-substrate Interactions. If stabilization by the amino acidic residues in the active site is not responsible for the easier leaving-group departure calculated for LgtC when compared to α1,3-GalT, other explanations need to be found. An analysis of the stabilization provided by the substrates themselves (inter-substrate interactions) during the cleavage of the O3B$_{UDP}$–C1′$_{\alpha\text{-Gal}}$ bond was then performed. In particular, the contribution of the acceptor substrate (LAT) was calculated. As Figure 5B shows, the electrostatic contribution of LAT to the stabilization of the QM region along the d(O3B$_{UDP}$–C1′$_{\alpha\text{-Gal}}$) bond-cleavage coordinate is completely different between the two enzymes: in LgtC, the inter-substrate interaction of UDP–Gal with LAT clearly facilitates the cleavage of the glycosidic bond, whereas in α1,3-GalT, it slightly destabilizes it. Thus, the different orientation of the acceptor substrate in the active site of these enzymes is conditioning not only their specificity (α1–3 and α1–4 in α1,3-GalT and LgtC, respectively) but also their ability to assist O3B$_{UDP}$–C1′$_{\alpha\text{-Gal}}$ bond breakage. A detailed analysis of the stabilizing role follows.

Substrate-Assisted Catalysis in α1,3-GalT and LgtC. According to the above analysis, α1,3-GalT needs a strong nucleophile because, contrary to what is found in LgtC, UDP is a bad leaving group as LAT is not able to stabilize initial UDP–Gal bond cleavage in α1,3-GalT. However, this nucleophilic assistance is not enough to achieve the reported reaction rate (which is of the same order as that of LgtC) and new interactions must be formed during galactosyl transfer. In our work on LgtC several substrate–substrate interactions were identified to promote reaction,[8] some of them involving LAT (Figure 6): a hydrogen bond between O2′$_{\alpha\text{-Gal}}$ and the UDP β-phosphate (O1B$_{UDP}$), a hydrogen bond between O3B$_{UDP}$ and the O4$_{\beta\text{-Gal}}$ attacking hydroxyl of LAT, and a hydrogen bond between O3B$_{UDP}$ and the O3$_{\beta\text{-Gal}}$ hydroxyl (adjacent to the attacking O4$_{\beta\text{-Gal}}$). In α1,3-GalT only the O2′$_{\alpha\text{-Gal}}$–O1B$_{UDP}$ hydrogen bond and the one of O3B$_{UDP}$ with the attacking hydroxyl (now O3$_{\beta\text{-Gal}}$) are possible. Nonetheless, the stabilization by O3$_{\beta\text{-Gal}}$(LgtC) was estimated to be ∼2 kcal/mol,[8] which is not enough to explain the differences observed

dx.doi.org/10.1021/ja4024447 | J. Am. Chem. Soc. 2013, 135, 7053–7063

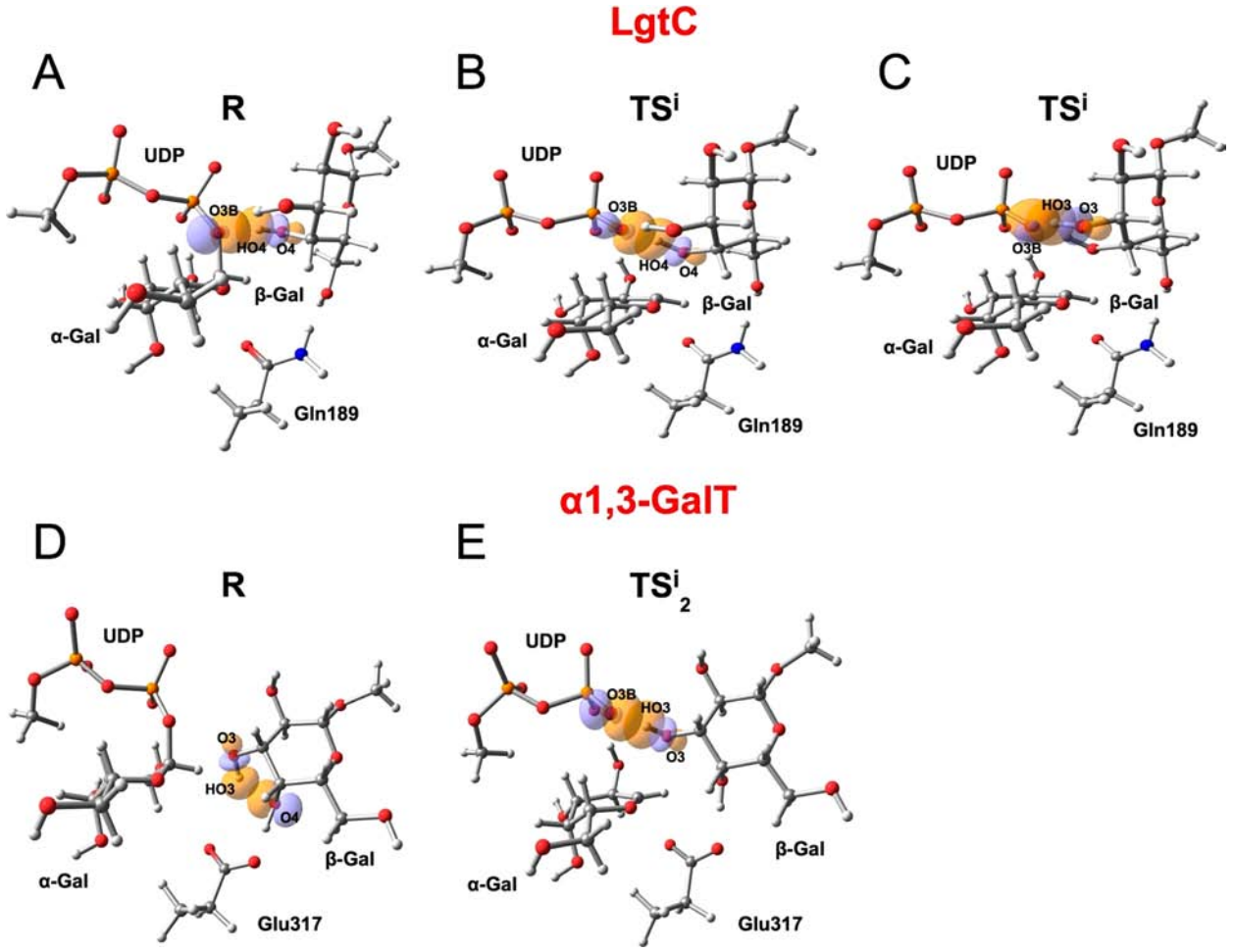

Figure 7. Interactions between molecular orbitals of the substrates relevant in galactosyl transfer according to a NBO analysis. These interactions involve, for LgtC, $O3B_{UDP}$ and the incoming $O4_{\beta\text{-Gal}}$ in the reactants (A) and in the S_Ni transition state (B), or the neighboring hydroxyl ($O3_{\beta\text{-Gal}}$), here only shown in the TS^i transition state (C); for α1,3-GalT, $O3_{\beta\text{-Gal}}$ interacts with $O4_{\beta\text{-Gal}}$ in the reactants (D) and with $O3B_{UDP}$ in the $TS^i{}_2$ transition state (E). For clarity, just a fraction of the QM atoms is shown.

in Figure 5A. Interestingly, we have found that the $O3B_{UDP}$−$HO4_{\beta\text{-Gal}}$ (LgtC) interaction is present both at the TS and at the reactants, whereas the equivalent $O3B_{UDP}$−$O3_{\beta\text{-Gal}}$ (α1,3-GalT) hydrogen bond is formed along the galactosyl transfer so that it is not present to stabilize the beginning of the bond breakage process (e.g., $d(HO3_{\beta\text{-Gal}}$−$O3B_{UDP})$ = 4.06 Å in R and ∼1.6 Å at the TSs, see Table 1). Therefore, the initial orientation of $HO3_{\beta\text{-Gal}}$ can be at the origin of the differences observed in UDP−Gal bond cleavage between α1,3-GalT and LgtC. To test this hypothesis we forced a hydrogen bond between $O3_{\beta\text{-Gal}}$ and $O3B_{UDP}$ in the reactants of α1,3-GalT and calculated again the energy for breaking the UDP−Gal bond (SI, Figure S5). Comparing with Figure 5A, it can be seen that when the $HO3_{\beta\text{-Gal}}$ is initially facing its final acceptor the leaving group is more easily released as the developing negative charge on UDP gets stabilized from the beginning, thus confirming our hypothesis.

A detailed study of the magnitude and nature of these inter-substrate interactions in galactosyl transfer by α1,3-GalT and LgtC was then carried out by a full donor−acceptor NBO analysis where the putative nucleophiles were also included (SI, Table S10). The previously characterized TS for LgtC[8] and the equivalent one for α1,3-GalT, more specifically the $TS^i{}_2$ obtained for the front-side attack mechanism, have been compared. Some catalytically relevant interacting molecular orbitals are depicted in Figure 7.

Three main conclusions can be outlined from the results. First, the largest contributions to TS stabilization involve interactions of the incoming hydroxyl group from LAT ($O4_{\beta\text{-Gal}}$ and $O3_{\beta\text{-Gal}}$ in LgtC and α1,3-GalT, respectively) with the final acceptor of the proton, $O3B_{UDP}$ (Figure 7B,E). Interestingly, a interaction between $O4_{\beta\text{-Gal}}$ (LgtC)/$O3_{\beta\text{-Gal}}$(α1,3-GalT) and a molecular orbital involving $(C1'-O5')_{\alpha\text{-Gal}}$ is also seen to participate in TS stabilization (SI, Figure S6A,B). In the case of LgtC, the interaction of the neighboring hydroxyl group with $O3B_{UDP}$ mentioned above is also highlighted in the analysis (Table S10, Figures 7C and S7A). Second, it is confirmed that a major difference between the two enzymes is that this hydrogen bond between $O3B_{UDP}$ and $O4_{\beta\text{-Gal}}$(LgtC)/$O3_{\beta\text{-Gal}}$(α1,3-GalT) is already present in the reactants only for LgtC. In the α1,3-GalT reactants, $O3_{\beta\text{-Gal}}$ is facing the neighboring $O4_{\beta\text{-Gal}}$ group, which in turn is hydrogen-bonded to $OE1_{E317}$ (Figure S7B). This network of hydrogen bonds was observed along all the MM and QM/MM MDs performed during the present study, suggesting that it is actually present in the Michaelis complex. It is thus a consequence of the substrates' binding orientation and interactions. This explains why $O3B_{UDP}$−$C1'_{\alpha\text{-Gal}}$ bond cleavage, described only by the $d(O3B_{UDP}$−$C1'_{\alpha\text{-Gal}})$ coor-

dx.doi.org/10.1021/ja4024447 | J. Am. Chem. Soc. 2013, 135, 7053−7063

dinate, is initially more difficult in α1,3-GalT than in LgtC (despite the assistance by Glu317 in the former). It would also explain why the $d(HO3_{\beta\text{-Gal}}-O3B_{UDP})$ had to be explicitly included in the RC for both the front-side attack and the double-displacement mechanisms, even though it is not until the second step when the transfer of $HO3_{\beta\text{-Gal}}$ to $O3B_{UDP}$ takes place (see Table 1 and Figure S8). During the sugar transfer reaction, reorientation of the incoming hydroxyl to form the $O3_{\beta\text{-Gal}}-O3B_{UDP}$ hydrogen bond will facilitate UDP departure and lead to energy barriers of the same order for both enzymes. Finally, contributions from the nucleophiles to TSs stabilization have also been identified and are quantified to be comparatively much less important than those from the inter-substrate interactions, especially in LgtC. In the case of α1,3-GalT, the stabilizing effect of Glu317 is more substantial (~7 kcal/mol, see Table S10).

Trapping a Covalent Intermediate (CGE)? The results presented so far suggest that both the front-side attack and the double-displacement mechanism could be operating at the same time and with similar rates in galactosyl transfer catalyzed by α1,3-GalT. Moreover, both mechanisms would require the presence of Glu317 and, more importantly, a substrate-assisted catalysis by the acceptor molecule in order to stabilize the increasing negative charge on UDP and achieve the reported k_{cat} values. The described substrate-assisted catalysis implies that, in the absence of the acceptor, formation of the covalent intermediate would not be possible (or extremely slow), which could explain why it is being so difficult to isolate such CGE. In fact, it is important to notice that even in the presence of LAT the CGE formation would be quite endoergic (11.4 ± 4.2 kcal/mol over the reactants) and that the CGE could easily go back to reactants (reverse barrier of 3.7 ± 1.3 kcal/mol).

We have further studied the importance of the acceptor in CGE formation by calculating the QM/MM energy profile leading to the CGE in the absence of LAT. For that, we removed LAT from the Michaelis complex, resolvated the resulting binary complex and reequilibrated the system (water molecules first, also the protein side chains afterward) by a 2 ns MM(CHARMM) MD. Three snapshots were randomly taken as starting points in the following QM/MM calculations (Figure 8). The corresponding energy profiles have high energy barriers (~30−38 kcal/mol) and are much more endoergic than when LAT is present (>10 kcal/mol). Dissociation of the CGE back to reactants has a barrier of only ~5 kcal/mol. All together, these results confirm our hypothesis.

Why is not Glu317 such a strong nucleophile as primarily expected in α1,3-GalT? Interestingly, if the system is not resolvated after LAT removal, so that the nucleophile only interacts with the α-Gal, CGE formation is "artificially" observed when the UDP−Gal bond is broken following the RC = $d(O3B_{UDP}-C1'_{\alpha\text{-Gal}})$ (SI, Figures S9A and S10A). Therefore, interaction of Glu317 with LAT or with water molecules seems to be reducing its nucleophilic character. Again, a NBO analysis of the different scenarios provides an explanation for this (SI, Table S11). As mentioned before, when LAT is present in the active site there is a hydrogen bond between $O4_{\beta\text{-Gal}}$ and $OE1_{E317}$; as a result of that, the $(CD-OE2)_{E317}$ bond acquires a double bond character and the negative charge on $OE2_{E317}$ is relatively moderate (Figure 9A). In this context, the antibonding (BD*) $(C1'-O5')_{\alpha\text{-Gal}}$ molecular orbital interacts with molecular orbitals of the Glu317 with a total interaction energy of 1.12 kcal/mol in favor of UDP departure (for $d(O3B_{UDP}-C1'_{\alpha\text{-Gal}})$ = 2.81 Å). When

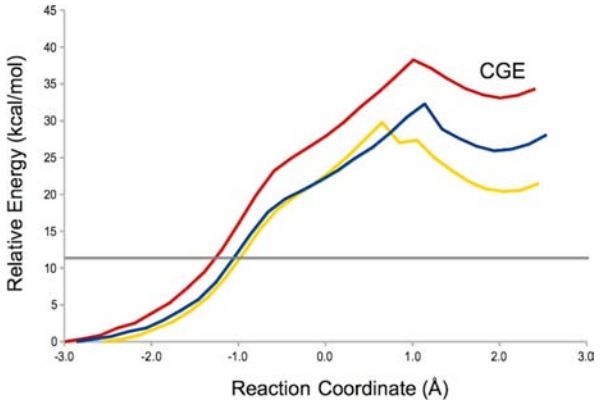

Figure 8. QM(M05-2X/TZVP//BP86/SVP)/CHARMM energy profiles for CGE formation when the acceptor LAT is not in the active site of α1,3-GalT. Reaction coordinate (RC) = $d(O3B_{UDP}-C1'_{\alpha\text{-Gal}}) - d(OE2_{E317}-C1'_{\alpha\text{-Gal}})$. Three different snapshots from a MD simulation were considered. The line at 11.4 kcal/mol indicates the average energy of the CGE formed in the original ternary complex (with LAT).

LAT is removed and the system resolvated, some water molecules come to interact with Glu317 and a similar scenario is found (Figure 9B) but with a less significant interaction energy (0.29 kcal/mol, for $d(O3B_{UDP}-C1'_{\alpha\text{-Gal}})$ = 2.89 Å). However, in the absence of the acceptor substrate and water molecules the $(CD-OE2)_{E317}$ bond would no longer have a double-bound character (the $(CD-OE1)_{E317}$ bond has) and the $OE2_{E317}$ atom that is facing the anomeric center would exhibit a higher negative charge. In this case, stronger interactions would be established between Glu317 and α-Gal (16.9 kcal/mol, at $d(O3B_{UDP}-C1'_{\alpha\text{-Gal}})$ = 2.89 Å, Figure 9C). Thus, in this context, Glu317 is assuming a more efficient role in the leaving-group departure so that, as mentioned above, the CGE would be readily formed (Figures S9A and S10A).

Therefore, this analysis shows that the nucleophilic strength of Glu317 in α1,3-GalT is reduced by its interaction with LAT so that Glu317 alone cannot promote the formation of a covalent intermediate and substrate-assisted catalysis (curiously by the same LAT) is required. Moreover, the interaction of Glu317 with water molecules also reduces its nucleophilic character. We then suggest that, along with the endoergicity for CGE formation and its low stability, these are the reasons why a covalent intermediate is not experimentally detected for the WT enzyme, even in the absence of LAT.

Mechanistic Implications for Retaining GTs. The detailed understanding of the reaction mechanism and the substrate−enzyme interactions in GHs has led to important developments, such as new drugs[59] or engineered GHs for synthetic or biotechnological applications.[60−62] The reaction mechanism used by GTs, though, has been a subject of debate for more than a decade and still remains an open question.[11,2] By analogy with retaining GHs, and despite an evident lack of evolutionary relatedness,[11] retaining GTs were first assumed to follow a double-displacement mechanism with formation of a CGE. However, structural data have shown that only very few enzymes, namely family GT6, have a suitably positioned nucleophilic residue.[2] Therefore, it is most likely that most retaining GTs follow an alternative mechanism. Both experimental and theoretical studies are now showing that the proposed front-side attack mechanism is perfectly feasible.[4−6,8,9,15] Still, it is unclear if GT6 family members use

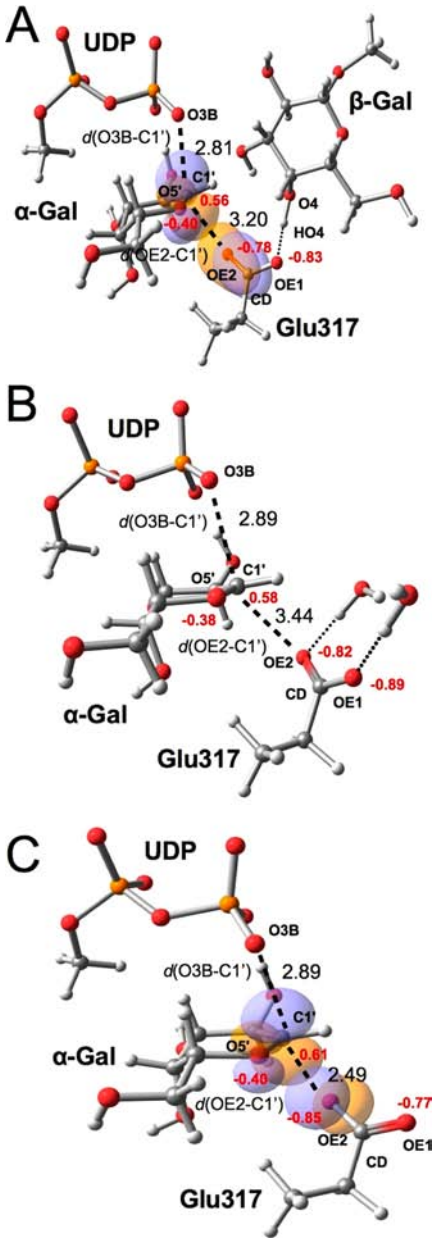

Figure 9. Structures along the UDP−Gal bond-breakage process (RC = $d(O3B_{UDP}-C1'_{\alpha\text{-Gal}})$) at the QM(M05-2X/TZVP// BP86/SVP// CHARMM level for α1,3-GalT (A) in the ternary complex, (B) when the system is resolvated after removing LAT, and (C) when LAT is removed from the reactants. Atomic charges (au) and distances (Å) are indicated in red and black respectively. For clarity, just a fraction of the QM atoms is shown. Molecular orbitals from the NBO analysis involving the Glu317 and the anomeric center (C1′) are also depicted in A and C.

the double-displacement strategy. In the present study we have shown that for α1,3-GalT (GT6) both alternatives could be taken place at the same time, as similar barrier heights have been calculated for the two mechanisms. Moreover, the front-side attack would be nucleophilically assisted by Glu317 and both mechanisms would require substrate-assisted catalysis to stabilize the negative charge on the leaving group to proceed at reliable rates. In fact, inter- or intra-substrate interactions that facilitate reaction are being described for both retaining and inverting GTs.[2,6,8,58,63] Apparently, different GTs could be using different substrate−substrate interactions to promote reaction depending on the nature and the relative orientation of their ligands.

What is emerging as a common inter-substrate interaction in all retaining GTs is an hydrogen bond between the β-phosphate and the attacking hydroxyl of the acceptor molecule (Figure 6, $O3_{\beta\text{-Gal}}$ in α1,3-GalT and $O4_{\beta\text{-Gal}}$ in LgtC). The latest theoretical and experimental works on retaining GTs[4−6,8,9,63,65,66] have confirmed that the final accepting base for the proton is the same phosphate and support the existence of such a hydrogen bond at the transition state. For LgtC (GT-A fold) this hydrogen bond is already present in the reactants.[8] For OtsA (GT-B), the interaction in the reactants is with another oxygen of the β-phosphate, and its reorientation toward the glycosidic oxygen has been suggested to be a driving force for the reaction.[6] In α1,3-GalT, this inter-substrate interaction is missing in the reactants but will be formed along the galactosyl transfer. The reason for this is that in the reactants $O3_{\beta\text{-Gal}}$ is making a hydrogen bond with $O4_{\beta\text{-Gal}}$, which is in turn hydrogen bonded to $OE1_{Glu317}$. We propose that, as a consequence of this, α1,3-GalT requires the presence of a nucleophile (Glu317) in the β-face of UDP−Gal to assist initial leaving-group departure. The presence of Glu317, which is also involved in proper binding of LAT, opens the door to the possibility of a double-displacement mechanism. However, even the double displacement needs the $O3B_{UDP}$−$HO3_{\beta\text{-Gal}}$ interaction as the nucleophilic strength of Glu317 is compromised by its interaction with $O4_{\beta\text{-Gal}}$. Therefore, and contrary to what has recently been proposed on the basis of model compounds,[7] our results suggest that the tight coordination of the pyrophosphate by positively charged residues is not enough and that substrate-assisted catalysis by the sugar acceptor hydroxyl group is required to achieve the observed reaction rates for retaining GTs. According to our calculations, proton transfer will not occur until the end of the reaction, but a tight hydrogen bond with the glycosidic oxygen needs to be formed earlier to allow leaving-group departure, even if a nucleophile is present.

From the enzyme's point of view, the use of the acceptor substrate to promote donor−glycosidic bond cleavage imposes that reaction will only be initiated (at suitable rates) once the ternary complex will be formed. This could be a way to slow down undesired hydrolysis in retaining GTs. In α1,3-GalT, hydrolysis of the donor substrate is 60-fold slower than the transfer reaction,[1] and for human ABO(H) blood group related retaining GTs, which also have a glutamate as a putative nucleophile, slow hydrolysis of the donor with retention of the configuration has been reported in the absence of the acceptor substrate.[3] In contrast, in retaining GHs, for which the double-displacement mechanism first proposed by Koshland[67] is generally accepted, hydrolysis is the target reaction. The difficulty of breaking the glycosidic bond between two sugars and the limited potential stabilization of the leaving-group departure by the acceptor substrate (a water molecule) are overcome by the implication of a protein residue acting as an acid catalyst that supplies the required proton to the leaving group. By doing this, CGE formation is made energetically accessible.[2] In transglycosidases,[68] the transfer of the monosaccharide follows a ping-pong mechanism; thus, the acceptor substrate is not present in the active site to cleave the glycosidic bond of the donor substrate, and a mechanism equivalent to the one used by retaining GHs has prevailed.

dx.doi.org/10.1021/ja4024447 | J. Am. Chem. Soc. 2013, 135, 7053−7063

CONCLUSIONS

The reaction mechanism used by retaining glycosyltransferases is still a matter of debate, and both experimental and theoretical scientists are trying to provide new knowledge to clarify this question. Here, QM(DFT)/MM calculations on the fully solvated enzyme have been used to shed light on this topic. By studying in detail galactosyl transfer catalyzed by α1,3-GalT and LgtC and comparing them, we have shown that LgtC binds the substrates in a relative orientation very convenient for catalysis, as substrate−substrate interactions can be readily established that efficiently participate in the stabilization of the β-phosphate negative charge (*substrate-assisted catalysis*). In contrast, the binding orientation and interactions that donor and acceptor must adopt in α1,3-GalT in order to achieve the desired reaction specificity (α1−3 linkage) reduce the number of interactions that facilitate initial UDP−Gal bond cleavage, requiring then a stronger nucleophile (Glu317) in the β-face of UDP−Gal to assist initial leaving-group departure (*nucleophilically assisted catalysis*). In particular, a hydrogen bond between the β-phosphate of the leaving group and the attacking hydroxyl of the acceptor molecule is not present in the α1,3-GalT Michaelis complex. However, pushing by Glu317 is not enough, but this hydroxyl will reorient during the reaction to form a hydrogen bond with the β-phosphate in the TS (TS stabilization) and finally result in similar energy barriers for both enzymes. The presence of a nucleophile in this GT6 family enzyme, Glu317, which is also an important determinant of acceptor binding, introduces the possibility of a double-displacement mechanism for this family. However, and according to our results, both the front-side attack (which seems to be the mechanism used by the other retaining GT families) and the double-displacement mechanisms could be taking place in α1,3-GalT with similar rates. In both mechanisms, substrate-assisted catalysis is required to proceed at reliable rates due to the reduced nucleophilic strength of Glu317 as a result of its interactions with the acceptor substrate (or with water molecules in the binary complex). The foregoing could be a strategy to avoid undesired hydrolysis of the donor substrate and, together with its limited stability, would also explain why it is so difficult to isolate a glycosyl−enzyme covalent intermediate.

ASSOCIATED CONTENT

Supporting Information

Methodological details, further QM/MM results, complete refs 17, 40, and 41, and optimized geometries of the 36 stationary points obtained in the present study (in pdb format). This material is available free of charge via the Internet at http://pubs.acs.org.

AUTHOR INFORMATION

Corresponding Author

laura.masgrau@uab.cat

Notes

The authors declare no competing financial interest.

ACKNOWLEDGMENTS

We thank the financial support from the Spanish "Ministerio de Economía y Competitividad" through project CTQ2011-24292 and the "Ramon y Cajal" program (L.M.), and from the "Generalitat de Catalunya", project 2009SGR409.

REFERENCES

(1) Monegal, A.; Planas, A. *J. Am. Chem. Soc.* **2006**, *128*, 16030−16031.
(2) Lairson, L. L.; Henrissat, B.; Davies, G. J.; Withers, S. G. *Annu. Rev. Biochem.* **2008**, *77*, 521−555.
(3) Soya, N.; Shoemaker, G. K.; Palcic, M. M.; Klassen, J. S. *Glycobiology* **2009**, *19*, 1224−1234.
(4) Errey, J. C.; Lee, S. S.; Gibson, R. P.; Martinez-Fleites, C.; Barry, C. S.; Jung, P. M.; O'Sullivan, A. C.; Davis, B. G.; Davies, G. J. *Angew. Chem.* **2010**, *49*, 1234−1237.
(5) Lee, S. S.; Hong, S. Y.; Errey, J. C.; Izumi, A.; Davies, G. J.; Davis, B. G. *Nat. Chem. Biol.* **2011**, *7*, 631−638.
(6) Ardèvol, A.; Rovira, C. *Angew. Chem.* **2011**, *50*, 10897−10901.
(7) Chan, J.; Tang, A.; Bennet, A. J. *J. Am. Chem. Soc.* **2012**, *134*, 1212−1220.
(8) Gómez, H.; Polyak, I.; Thiel, W.; Lluch, J. M.; Masgrau, L. *J. Am. Chem. Soc.* **2012**, *134*, 4743−4752.
(9) Gómez, H.; Lluch, J. M.; Masgrau, L. *Carbohydr. Res.* **2012**, *356*, 204−208.
(10) Díaz, A.; Díaz-Lobo, M.; Grados, E.; Guinovart, J. J.; Fita, I.; Ferrer, J. C. *IUBMB Life* **2012**, *64*, 649−658.
(11) Davies, G. J.; Withers, S. G. In *Comprehensive Biological Catalysis*; Sinnott, M. L., Ed.; Academic: London, 1998; pp 119−208.
(12) Lairson, L. L.; Chiu, C. P.; Ly, H. D.; He, S.; Wakarchuk, W. W.; Strynadka, N. C.; Withers, S. G. *J. Biol. Chem.* **2004**, *279*, 28339−28344.
(13) Molina, P.; Knegtel, R. M.; Macher, B. A. *Biochim. Biophys. Acta* **2007**, *1770*, 1266−1273.
(14) Zhang, Y.; Swaminathan, G. J.; Deshpande, A.; Boix, E.; Natesh, R.; Xie, Z.; Acharya, K. R.; Brew, K. *Biochemistry* **2003**, *42*, 13512−13521.
(15) Tvaroška, I. *Carbohydr. Res.* **2004**, *339*, 1007−1014.
(16) Humphrey, W.; Dalke, A.; Schulten, K. *J. Mol. Graph.* **1996**, *14*, 33−38.
(17) MacKerell, A. D., Jr.; et al. *J. Phys. Chem. B* **1998**, *102*, 3586−3616.
(18) MacKerell, A. D., Jr.; Feig, M.; Brooks, C. L. *J. Am. Chem. Soc.* **2004**, *126*, 698−699.
(19) MacKerell, A. D. J.; Brooks, C. III; Nilsson, L.; Roux, B.; Won, Y.; Karplus, M. In *The Encyclopedia of Computational Chemistry*; Schleyer, P. v. R., Ed.; John Wiley & Sons: Chichester, 1998; pp 271−277.
(20) Phillips, J. C.; Braun, R.; Wang, W.; Gumbart, J.; Tajkhorshid, E.; Villa, E.; Chipot, C.; Skeel, R. D.; Kalé, L.; Schulten, K. *J. Comput. Chem.* **2005**, *26*, 1781−1802.
(21) Guvench, O.; Hatcher, E. R.; Venable, R. M.; Pastor, R. W.; Mackerell, A. D., Jr. *J. Chem. Theory Comput.* **2009**, *5*, 2353−2370.
(22) Elstner, M.; Porezag, D.; Jungnickel, G.; Elsner, J.; Haugk, M.; Frauenheim, T.; Suhai, S.; Seifert, G. *Phys. Rev. B* **1998**, *58*, 7260−7268.
(23) Frauenheim, T.; Seifert, G.; Elstner, M.; Niehaus, T.; Köhler, C.; Amkreutz, M.; Sternberg, M.; Hajnal, Z.; Carlo, A. D.; Suhai, S. *J. Phys.: Condens. Matter* **2002**, *14*, 3015−3047.
(24) Slater, J. C. *Phys. Rev.* **1951**, *81*, 385−390.
(25) Vosko, S. H.; Wilk, L.; Nusair, M. *Can. J. Phys.* **1980**, *58*, 1200−1211.
(26) Becke, A. D. *Phys. Rev. A* **1988**, *38*, 3098−3100.
(27) Perdew, J. P. *Phys. Rev. B* **1986**, *33*, 8822−8824.
(28) Schäfer, A.; Horn, H.; Ahlrichs, R. *J. Chem. Phys.* **1992**, *97*, 2571−2577.
(29) Eichkorn, K.; Treutler, O.; Öhm, H.; Häser, M.; Ahlrichs, R. *Chem. Phys. Lett.* **1995**, *240*, 283−289.
(30) Eichkorn, K.; Welgend, F.; Treutler, O.; Ahlrichs, R. *Theor. Chem. Acc.* **1997**, *97*, 119−124.
(31) Zhao, Y.; Schultz, N. E.; Truhlar, D. G. *J. Chem. Theory Comput.* **2006**, *2*, 364−382.
(32) Schäfer, A.; Huber, C.; Ahlrichs, R. *J. Chem. Phys.* **1994**, *100*, 5829−5835.
(33) Kóňa, J.; Tvaroška, I. *Chem. Pap.* **2009**, *63*, 598−607.

(34) Gábor, I. C.; Alfred, D. F.; Glenn, P. J.; Carlos, A. S. *J. Chem. Theory Comput.* **2009**, *5*, 679−692.
(35) Foster, J. P.; Weinhold, F. *J. Am. Chem. Soc.* **1980**, *102*, 7211−7218.
(36) Reed, A. E.; Weinhold, F. *J. Chem. Phys.* **1983**, *78*, 4066−4073.
(37) Reed, A. E.; Weinstock, R. B.; Weinhold, F. *J. Chem. Phys.* **1985**, *83*, 735−746.
(38) Reed, A. E.; Curtiss, L. A.; Weinhold, F. *Chem. Rev.* **1988**, *88*, 899−926.
(39) Glendening, E. D.; Reed, A. E.; Carpenter, J. E.; Weinhold, F. *NBO* Version 3.1.
(40) Frisch, M. J.; et al. *Gaussian09*, revision A.1; Gaussian, Inc.: Wallingford, CT, 2009.
(41) Sherwood, P.; et al. *J. Mol. Struct. (Theochem.)* **2003**, *632*, 1−28.
(42) Ahlrichs, R.; Bär, M.; Häser, M.; Horn, H.; Kölmel, C. *Chem. Phys. Lett.* **1989**, *162*, 165−169.
(43) Becke, A. D. *J. Chem. Phys.* **1993**, *98*, 5648−5652.
(44) Stephens, P. J.; Devlin, F. J.; Chabalowski, C. F.; Frisch, M. J. *J. Phys. Chem.* **1994**, *98*, 11623−11627.
(45) Lee, C. T.; Yang, W. T.; Parr, R. G. *Phys. Rev. B: Condens. Matter* **1988**, *37*, 785−789.
(46) Thiel, W. *MNDO99*, version 7.0; Max-Planck-Institut für Kohlenforschung: Mülheim an der Ruhr, Germany, 2005.
(47) Smith, W.; Forester, T. R. *J. Mol. Graph.* **1996**, *14*, 136−141.
(48) Dirk, B.; Walter, T. *J. Phys. Chem.* **1996**, *100*, 10580−10594.
(49) de Vries, A. H.; Sherwood, P.; Collins, S. J.; Rigby, A. M.; Rigutto, M.; Kramer, G. J. *J. Phys. Chem. B* **1999**, *103*, 6133−6141.
(50) Sherwood, P.; de Vries, A. H.; Collins, S. J.; Greatbanks, S. P.; Burton, N. A.; Vincent, M. A.; Hillier, I. H. *Faraday Discuss.* **1997**, *106*, 79−92.
(51) Nocedal, J. *Math. Comp.* **1980**, *35*, 773−782.
(52) Liu, D. C.; Nocedal, J. *Math. Programming* **1989**, *45*, 503−528.
(53) Banerjee, A.; Adams, N.; Simons, J.; Shepard, R. *J. Phys. Chem.* **1985**, *89*, 52−57.
(54) Baker, J. *J. Comput. Chem.* **1986**, *7*, 385−395.
(55) Billeter, S. R.; Turner, A. J.; Thiel, W. *Phys. Chem. Chem. Phys.* **2000**, *2*, 2177−2186.
(56) Thomas, A.; Field, M. J. *J. Am. Chem. Soc.* **2002**, *124*, 12342−12438.
(57) Poulsen, T. D.; Garcia-Viloca, M.; Gao, J.; Truhlar, D. G. *J. Phys. Chem. B* **2003**, *107*, 9567−9578.
(58) Zhang, Y.; Wang, P. G.; Brew, K. *J. Biol. Chem.* **2001**, *276*, 11567−11574.
(59) von Itzstein, M.; Wu, W.; Kok, G. B.; Pegg, M. S.; Dyason, J. C.; Jin, B.; Phan, T. V.; Smythe, M. L.; White, H. F.; Oliver, S. W.; Colman, P. M.; Varghese, J. N.; Ryan, D. M.; Woods, J. M.; Bethell, R. C.; Hotham, V. J.; Cameron, J. M.; Penn, C. R. *Nature* **1993**, *363*, 418−423.
(60) Mackenzie, L. F.; Wang, Q.; Warren, R. A. J.; Withers, S. G. *J. Am. Chem. Soc.* **1998**, *120*, 5583−5584.
(61) Malet, C.; Planas, A. *FEBS Lett.* **1998**, *440*, 208.
(62) Moracci, M.; Tricone, A.; Perugino, G.; Ciaramella, M.; Rossi, M. *Biochemistry* **1998**, 17262.
(63) Persson, K.; Ly, H. D.; Dieckelmann, M.; Wakarchuk, W. W.; Withers, S. G.; Strynadka, N. C. *Nat. Struct. Biol.* **2001**, *8*, 166−175.
(64) Tvaroška, I.; Kozmon, S.; Wimmerová, M.; Koca, J. *J. Am. Chem. Soc.* **2012**, *134*, 15563−15571.
(65) Tvaroška, I. *Carbohydr. Res.* **2004**, *339*, 1007−1014.
(66) André, I.; Tvaroška, I.; Carver, J. P. *Carbohydr. Res.* **2003**, *338*, 865−877.
(67) Koshland, D. E. *Biol. Rev. Camb. Philos. Soc.* **1953**, *28*, 416−36.
(68) Amaya, M. F.; Watts, A. G.; Damager, I.; Wehenkel, A.; Nguyen, T.; Buschiazzo, A.; Paris, G.; Frasch, A. C.; Withers, S. G.; Alzari, P. M. *Structure* **2004**, *12*, 775−784.